論文 Analysis of Size Effect in Concrete Structures

Ahmed Saad Eldin MORGAN*1, and Junichiro NIWA*2

ABSTRACT: In this paper the size effect in concrete and reinforced concrete structures is predicted by computer simulation of failures using the program **ANACS** (Advanced Nonlinear Analysis of Concrete Structures). The material model is based on the fictitious crack modeling with two orthogonal rod elements. The fracture of concrete is modeled based on the fracture energy-related softening. This enables a modeling of the size effect in cases of flexure and shear types of failure in concrete and reinforced concrete structures. Using the arc-length method post peak behavior can be predicted well even for snap back instability. Examples of flexure failure of plain concrete beams, and shear failure of reinforced concrete beams are shown.

KEY WORDS: concrete fracture, size effect, finite element, discrete model, fictitious crack, plain concrete, reinforced concrete, flexure strength, shear strength.

1. INTRODUCTION

The size effect is defined through a comparison of geometrically similar structures of different sizes. A dependence of nominal stress at ultimate load on the structure size is called the size effect. Thus, for example the tensile failure of concrete cannot be described by the tensile strength only. Then, the size effect is for design engineer probably the most compelling reason for using fracture mechanics. The tensile fracture is clearly a process of structure failure, where a discrete crack is formed in continuum and its solution is dependent on loading and boundary conditions. This process can be described by the fictitious crack model with two perpendicular rod elements, which imply the localization of crack [1]. The advantage of this formulation is that it solves a problem of discontinua with the help of the standard finite element method. In fact, lumping all nonlinear deformation into interface elements involves a mechanism of softening lines or softening hinges to be assumed, similar to the assumption of yield lines or plastic hinges in the theory of plasticity.

The authors have shown that the fictitious crack model combined with arc-length model is capable of describing the size effect even in post peak brittle failure in flexure and shear problems in concrete and reinforced concrete beams, respectively. The present paper documents these experiences on calculations made in connection with JSCE provisions of size effect analysis in concrete structures. The comparison with experiments is not presented. However, such a comparison can be certainly done for the small size beams, but for the large size beams it is very difficult to perform the experiments.

2. FINITE ELEMENT MODELING FOR CONCRETE AND STEEL ELEMENTS

Complete detailed discussion of the **ANACS** program is exceeding the range of this paper, and therefore only main principles are mentioned here and a detail description is devoted only to

*1 Department of civil engineering, Nagoya University, Member of JCI
*2 Department of civil engineering, Nagoya University, DR, Member of JCI

the modeling of tensile fracture, which is prevailing in the analyzed cases. The ANACS program has a complete finite element armory which has 4,5,6,7, and 8 nodded quadrilateral elements.

Also, 3, and 6 nodded triangular elements have been incorporated into the program in order to provide for mesh grading and flexibility in mesh construction. Concrete elements are elastic in tension. Therefore, the flexure and shear cracks can be easily localized based on fictitious crack approach by using the two orthogonal rod elements. Concrete elements in compression is modeled by bi- linear stress strain curve as shown in **Fig.1.**

A two node truss element for steel simulation is proposed with a bilinear force-displacement relation **(Fig.2).** Each node of this element has two degrees of freedom. This element is connected directly to the concrete.

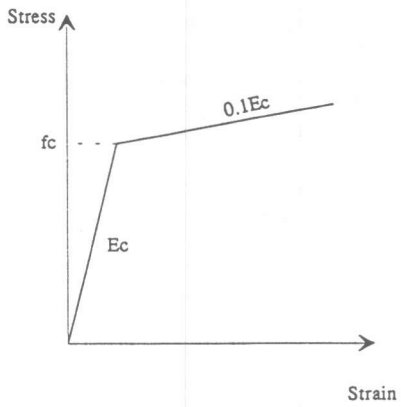

Fig. 1: Concrete model in compression

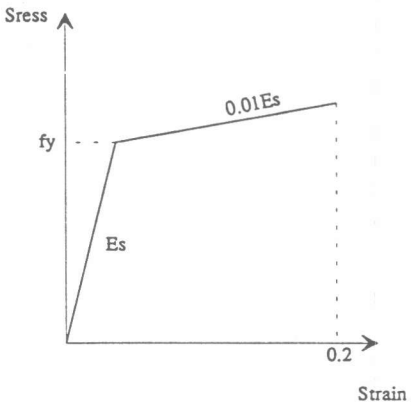

Fig. 2: Steel model

Due to the fact that the studied cases in this paper concern with flexural failure of plain concrete beams and diagonal tension failure of reinforced concrete beams, thus the stresses in both concrete and steel are always within the elastic range.

3. FICTITIOUS CRACK SIMULATION FOR CONCRETE

The two orthogonal rod elements **(Fig.3)** are used to simulate the crack and represent the localized crack zone. These rods exhibit non linear stress-strain behavior of concrete by using the 1/4th softening curve. For this concrete, the fracture energy remains constant and is equal to 100 (N/m) as recommended by experimental results. The length of the rod element is assumed as unity (L=1). The rod elements can be described as two nodes connected by two orthogonal rods which can be placed between coupled nodes of concrete element along the predefined crack path, and oriented at some angle θ relative to global coordinate system. The stiffness matrix of the rod element which perpendicular to the crack path is given using the force-displacement relation in the global system of axes as follows

$$\begin{bmatrix} F_x^i \\ F_y^i \\ F_x^j \\ F_y^j \end{bmatrix} = \frac{A_C E_R}{L} \begin{bmatrix} \cos\theta^2 & \sin\theta\cos\theta & -\cos\theta^2 & -\sin\theta\cos\theta \\ & \sin\theta^2 & -\sin\theta\cos\theta & -\sin\theta^2 \\ & & \cos\theta^2 & \sin\theta\cos\theta \\ Symmetry & & & \sin\theta^2 \end{bmatrix} \begin{bmatrix} u^i \\ v^i \\ u^j \\ v^j \end{bmatrix} \qquad (1)$$

Where: A_C is the area of concrete served by this rod element, and E_R is the stiffness of the rod element perpendicular to the crack.

Since the rod element which is parallel to the crack path is perpendicular to the other one, therefore the stiffness matrix for this rod element can be considered as $\cos(\theta+90°) = -\sin\theta$, $\sin(\theta+90°) = \cos\theta$, and G_C (shear modules of concrete) instead of E_R. Using the 1/4th model curve (Fig.4), the strain can be calculated which is equivalent to the crack width and then the corresponding stress can be obtained. Also, the compression bilinear curve is incorporated to the 1/4th tension model to simulate the rod element under compression as shown in Fig.4.

For the 1/4th tension model,

$$\varepsilon_p = \frac{f_t}{E_C} \qquad \varepsilon_1 = 0.75\frac{G_F}{f_t} \qquad \varepsilon_2 = 5\frac{G_F}{f_t} \tag{2}$$

$$\sigma = \begin{cases} E_C\varepsilon & 0 < \varepsilon \le \varepsilon_p \\ f_t - \dfrac{0.75f_t(\varepsilon-\varepsilon_p)}{\varepsilon_1-\varepsilon_p} & \varepsilon_p < \varepsilon \le \varepsilon_1 \\ \dfrac{f_t}{4} - \dfrac{f_t(\varepsilon-\varepsilon_1)}{4(\varepsilon_2-\varepsilon_1)} & \varepsilon_1 < \varepsilon \le \varepsilon_2 \\ 0 & \varepsilon_2 < \varepsilon \end{cases} \tag{3}$$

$$E_R = \begin{cases} E_C & 0 < \varepsilon \le \varepsilon_p \\ E_{Secant} & \varepsilon_p < \varepsilon \le \varepsilon_2 \\ 0.00001E_C & \varepsilon_2 < \varepsilon \end{cases} \tag{4}$$

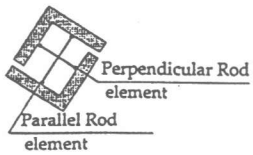

Fig.3 The rod elements for crack simulation

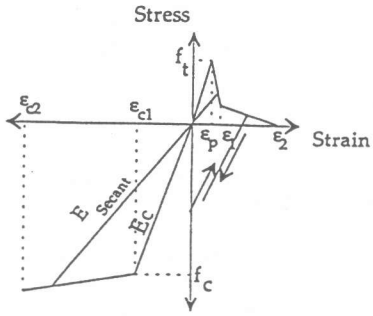

Fig.4 Stress-strain model for perpendicular rod element

For the compression model,

$$\sigma_{comp.} = -\begin{cases} E_C|\varepsilon_{c1}| & 0 < |\varepsilon| \le |\varepsilon_{c1}| \\ f'_c + 0.1E_C\left(\dfrac{|\varepsilon|-|\varepsilon_{c1}|}{|\varepsilon_{c2}|-|\varepsilon_{c1}|}\right) & |\varepsilon_{c1}| < |\varepsilon| \le |\varepsilon_{c2}| \\ 0 & |\varepsilon_{c2}| < |\varepsilon| \end{cases} \tag{5}$$

$$E_{comp.} = \begin{cases} E_C & 0 < |\varepsilon| \le |\varepsilon_{c1}| \\ E_{Secant} & |\varepsilon_{c1}| < |\varepsilon| \le |\varepsilon_{c2}| \\ 0.00001E_C & |\varepsilon_{c2}| < |\varepsilon| \end{cases} \tag{6}$$

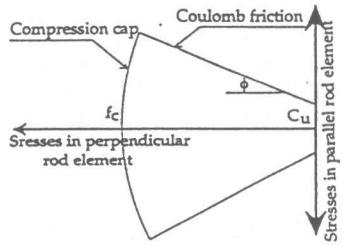

Fig.5 Failure criterion for rod elements in compression

Where f_t, and f'_c are the tensile and compressive strengths of concrete, respectively. G_F is the fracture energy of concrete, and E_C is the Young's modulus of concrete.

Also, to have a realistic model, unloading and reloading phenomenon was incorporated into the tension model.

The stress-strain relation for parallel rod element is taken as linear elastic till the tensile stress in the perpendicular rod element exceeds the tensile strength of concrete. Thus, when the crack starts at certain perpendicular rod element, the resistance of corresponding parallel rod element vanishes.

At advanced stages of fracture zone development, the compressive stress in the upper part of the beam becomes large, in both orthogonal rod elements, and in order to consider mode II of failure, the failure envelope that complies with a Coulomb type is adapted [4]. The Coulomb friction envelope of the model is shown in Fig.5, and the model is determined by the cohesion C_u, and the friction angle ϕ. If Coulomb friction occurs, the stresses in the perpendicular rod elements are vanishes.

4. NUMERICAL SOLUTION TECHNIQUE FOR NONLINEAR ANALYSIS

The current analysis is tried to trace the entire load-deformation response of the concrete structures. However, tracing of limit point and post limit path is notoriously difficult especially for structures which have a response involving a snap back behavior. However, it is important to know whether the structure collapse is of a ductile or brittle form, and to define a material modeling including the softening behavior. Since, the establishment of arc-length procedure [2] is for dealing with overcoming limit points in a nonlinear solution path. Moreover, a technique has been adopted [5] to maintain the symmetric banded nature of the equilibrium equations.

The basic idea in all arc-length methods is to modify the load level at each iteration, rather than holding the applied load level constant during a load step, so that the solution follows some specified path until convergence is attained.

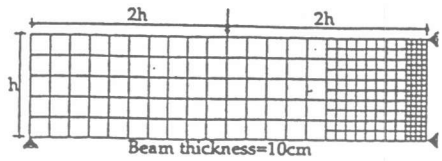

Fig.6 The mesh for plain concrete beams

5. TENSILE BENDING FAILURE OF PLAIN CONCRETE BEAMS

The concrete beam geometry is illustrated in Fig.6. Five different sizes are considered h=10, 50,100,200,300cm. Only symmetrical half of the beam was analyzed in order to avoid the reversible displacement after the crack begins to open which leads to numerical instability and lack of convergence through arc-length calculation procedure. Also, two perpendicular rod elements are incorporated through the bending crack. Actually, there is no shear stress along this flexure crack., but the incorporation of the rod element which parallel to crack path is needed to maintain the structure stability against any vertical forces produced by numerical calculations such as unbalanced forces. Also, as shown in Fig.6 both 4 nodded elements and side nodded transition 5 nodded elements are used to facilitate mesh grading. Further, it is noticed that the numerical instabilities through the calculations are reduced as much as we use rod elements along the crack path. Thus, the mesh was graded fine near the center line predefined crack, with 20 elements over the beam depth, and then 41 rod elements are used along the crack path with the help of 5 nodded transition element. The failure was initiated by formation of a crack process zone with a discrete crack in the region of tensile stresses. The solution was done by the arc-length control and was stable in all cases in the whole softening range as shown in Fig.7 which shows the load-displacement diagram of beam size 50cm with a post peak snap back response. Moreover, Fig.8 shows the tendency of

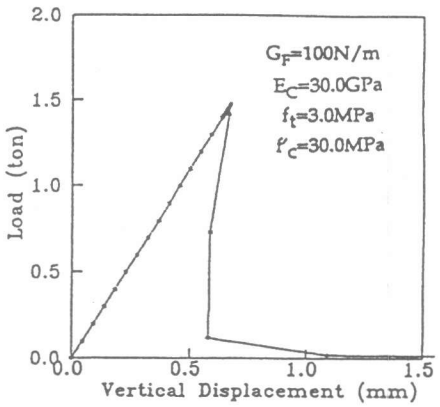

Fig.7 Load displacement diagram at loading point

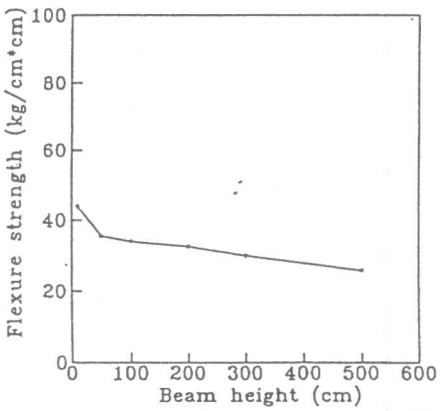

Fig.8 Size effect in flexural strength

ultimate strength to decrease with the increase of beam size. This behavior is known as the size effect. Also, as shown in **Fig.8** the size effect disappears for large depths, and the peak stress of the beams tends to become equal to tensile strength of concrete.

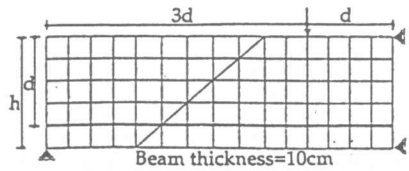

Fig.9 The mesh for reinforced concrete beams

6. SHEAR FAILURE OF REINFORCED CONCRETE BEAMS WITHOUT STIRRUPS

The geometry of the analyzed reinforced concrete beams is shown in **Fig.9** where both 6 nodded triangular elements, and 8 nodded quadrilateral elements are utilized. Six beam sizes are considered from 10 to 500cm. They are reinforced with the longitudinal bars at the effective depth d equal to 0.8 of the beam height. The beams are geometrically similar, the reinforcing ratio is 2%, and the ratio of shear span to depth of beam was set to 3.0. The concrete properties identical for all six beams are: f'_C=30.0MPa, f_t=3.0MPa, G_F=100N/m, E_C=30.0GPa. The reinforcement has the yield strength f_y=400.0MPa, and Young's modulus E_S=210.0GPa. The inclination of fictitious shear crack which gives the minimum shear strength is found equal to 40° and it is located at distance d from the support [1]. Fracture zone was modeled by force of rod elements between the pairs of decoupled nodes along a priori chosen crack path. The fracture softening properties of **Fig.10** shows that for large sizes such as h=100cm, failure becomes more brittle and the snap-back behavior occurs. The snap back phenomenon occurs because there is a sudden bifurcation process which leads to a sudden drop in both load and deflection. Also, the results of this study with design formula of JSCE are shown in **Fig.11**. According to this figure, the tendency of shear strength to decrease with the increase of the beam size has been obtained and shows the good agreement with JSCE design formula in small depths till 100cm. However, as shown in **Fig.11** the size effect disappears at large depths. Shear stresses across the fracture zone carried by aggregate interlocking between fracture surfaces were not considered, nor was the shear force carried by dowel action of the reinforced steel considered. These assumptions mean that calculated shear strengths become conservative. Furthermore, **Fig.12a** and **Fig.12b** show the deformed shapes at the peak load and at the next increment after the peak of the beam having 100cm height. It can be noticed that the displacements at beam axis of symmetry and around loading point in **Fig.12b** is smaller than that of **Fig.12a**, which illustrates the effect of snap back.

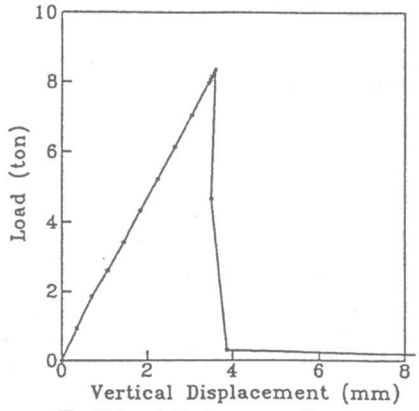

Fig.10 Load displacement diagram at loading point

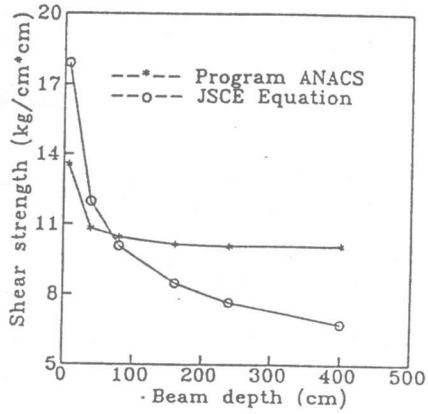

Fig.11 Comparison of shear strength analysis with ANACS program and JSCE equation

Based on extensive parametric study we found that the most appropriate C_u, and ϕ of Coulomb criterion in case of inclination of crack equal to 40° are 2.5 MPa, and 30°, respectively.

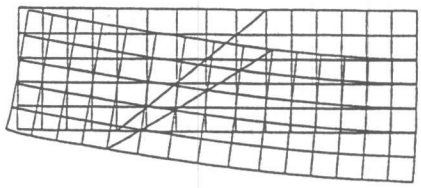

Fig.12a Deformed shape at the peak load

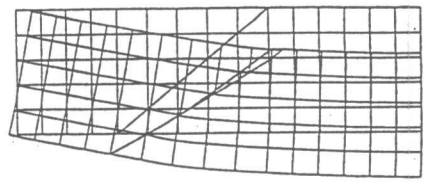

Fig.12b Deformed shape for the first increment after the peak load

7. CONCLUSIONS

It is possible to study the influence of different variables on flexure, and shear strength theoretically by means of nonlinear fracture mechanics. In particular, fracture mechanics offers a possibility to explain the size effect in both flexure and shear strengths. It was observed that for smaller beams till 100cm height the shear capacity of beams having only flexural reinforcement is profoundly affected by size effect. On the other hand, beams with height more than 100cm the numerical predictions showed that the size effect becomes negligible. Snapback phenomenon occurs when the beam size increases and the brittle behavior of concrete beams becomes more significant. The results of JSCE formula for shear is more or less conservative for large beams.

REFERENCES

1) Niwa, J., et al. "Size Effect Analysis for Shear Strength of Concrete Beams Based on Fracture Mechanics," J. of M.C.S.P. of JSCE, No. 508/V-26, 1995, Feb., pp.45-53.

2) Riks, E. "An Incremental Approach to the Solution of Snapping and Buckling Problems," Int. J. Solids Struct., 15, 1979, pp. 524-551.

3) Crisfield, M.A., "A Fast Incremental /Iterative Solution Procedure That Handles Snap-Through," Computers & Structures, Vol. 13, 1981, pp.55-62.

4) Rots, J.G., "Computational Modeling of Concrete Fracture," Heron, Vol. 34, No.1, 1988, pp. 335-350.

5) Batoz, J.L. and Dhatt, G., "Incremental Displacement Algorithms for Nonlinear Problems," Int. J. Num. Meth. Engng 14, 1979, pp.1262-1266.

6) Niwa, J., et al., "Revaluation of the Equation for Shear Strength of Reinforced Concrete Beams without Web Reinforcement," Concrete library of JSCE, No. 9., 1987, June, pp. 65-84.